

Reaction of $\text{CpW}(\text{CO})_2(\mu\text{-PPh}_2)\text{Mo}(\text{CO})_5$ and $\text{Fe}_2(\mu\text{-S}_2)(\text{CO})_6$: Unusual Fragmentation and Coordination of $\text{Fe}_2(\mu\text{-S}_2)(\text{CO})_6$

Md. Munkir Hossain, Hsiu-Mei Lin, and Shin-Guang Shyu*

Institute of Chemistry, Academia Sinica, Taipei, Taiwan 11529, Republic of China

Received March 11, 2004

Reaction of $\text{Fe}_2(\mu\text{-S}_2)(\text{CO})_6$ with $\text{CpW}(\text{CO})_2(\mu\text{-PPh}_2)\text{Mo}(\text{CO})_5$ at dichloromethane reflux afforded heterotrimetallic clusters $\text{CpW}(\mu\text{-PPh}_2)\text{Mo}(\text{CO})_3(\mu\text{-CO})(\mu_3\text{-S})_2\text{Fe}_2(\text{CO})_5$ (**1**), $\text{Cp}(\text{CO})\text{W}(\mu\text{-PPh}_2)\text{Mo}(\text{CO})_3(\mu_3\text{-S})_2\text{Fe}(\text{CO})_3$ (**2**), $\text{CpW}(\mu\text{-PPh}_2)\text{Mo}(\text{CO})_3(\mu_3\text{-S})_2\text{Fe}_2(\mu\text{-CO})(\text{CO})_4$ (**3**), and $\text{CpW}(\text{CO})(\mu_3\text{-S})_2\text{Fe}(\mu\text{-PPh}_2)\text{Fe}(\text{CO})_4\text{Mo}(\mu_3\text{-S})_2\text{Fe}_2(\text{CO})_6$ (**4**). Thermolysis of **1** in dichloromethane produced **3**, which was also obtained by the reaction of **2** with $\text{Fe}_2(\text{CO})_9$ at dichloromethane reflux. Reflux of a benzene solution of **3** with norbornadiene (nbd) produced $\text{CpW}(\mu\text{-PPh}_2)\text{Mo}(\text{CO})(\text{nbd})(\mu_3\text{-S})_2\text{Fe}_2(\mu\text{-CO})(\text{CO})_4$ (**5**), but the typical reaction without nbd afforded a benzene substitution product, $\text{CpW}(\mu\text{-PPh}_2)\text{Mo}(\eta^6\text{-C}_6\text{H}_6)(\mu_3\text{-S})_2\text{Fe}_2(\mu\text{-CO})(\text{CO})_4$ (**6**). Molecular structures of **1–6** were determined by single-crystal X-ray diffraction analyses. Cluster **1** has bitetrahedral geometry, where the Fe_2MoW core is intercepted by an Fe–W bond to FeMoW and Fe_2W units, and each unit is capped by a $\mu_3\text{-S}$ atom. Cluster **2** is a rare example of square pyramidal geometry with the FeS_2W plane capped by a Mo atom, whereas cluster **3** consists of an Fe_2MoW tetrahedron core with each FeMoW face capped by a $\mu_3\text{-S}$ atom. Clusters **4–6** possess an Fe_2MoW core geometry similar to that of **3**, where carbonyl ligands on the Mo site were replaced by $\text{Fe}_2(\mu\text{-S}_2)(\text{CO})_6$, nbd, and benzene, respectively.

Introduction

The simplest homo- and hetero-dichalcogens of iron carbonyl, $\text{Fe}_2(\mu\text{-EE}')(\text{CO})_6$ ($\text{E} = \text{E}'$ and $\text{E} \neq \text{E}'$; $\text{E}, \text{E}' = \text{S}, \text{Se}, \text{Te}$), are now well established.¹ Among them $\text{Fe}_2(\mu\text{-S}_2)(\text{CO})_6$, which was first reported by Hieber in 1958,^{1a} has been extensively investigated over the years.^{2–5} It has been used as a building block in cluster growth reactions, and the sulfur bridges in the resulting clusters provide extra stability. Its chemistry has been generally initiated by the sulfur atom, through cleavage of its potentially reactive S–S bond or utilization of lone pairs on sulfur atoms. Reactions have also been reported

that proceed through Fe–Fe bond scission.^{1b} Even its Fe–S linkage has been exploited for the synthesis of biologically related compounds that could mimic metalloenzymes involved in biological redox processes and in nitrogenase.⁶ Recently it has also been used to prepare macrocycles that contain butterfly transition metal cluster cores.⁷ The inorganic disulfide $\text{Fe}_2(\mu\text{-S}_2)(\text{CO})_6$ is very similar in reactivity to organic disulfides RSSR toward reduction of S–S bonds by sodium metal and by metal hydrides, nucleophilic cleavage by organolithium and Grignard reagents, and insertion of coordinatively unsaturated mononuclear low-valent transition metals.^{1b,5a,8} Insertion of single- and triple-bonded homodinuclear species into the S–S bond of $\text{Fe}_2(\mu\text{-S}_2)(\text{CO})_6$ has been also reported.⁹ In contrast, insertion reaction of such heterodinuclear species has not been

(1) (a) Hieber, W.; Gruber, J. Z. *Anorg. Allg. Chem.* **1958**, *296*, 91. (b) Seyferth, D.; Henderson, R. S.; Song, L.-C. *Organometallics* **1982**, *1*, 125. (c) Lesch, D. A.; Rauchfuss, T. B. *Inorg. Chem.* **1981**, *20*, 3583. (d) Mathur, P.; Chakraborty, D.; Hossain, Md. M.; Rashid, R. S.; Rugmini, V.; Rheingold, A. L. *Inorg. Chem.* **1992**, *31*, 1106. (e) Mathur, P.; Chakraborty, D.; Hossain, Md. M. *J. Organomet. Chem.* **1991**, *401*, 167. (f) Mathur, P.; Chakraborty, D.; Hossain, Md. M.; Rashid, R. S. *J. Organomet. Chem.* **1991**, *420*, 79.

(2) Whitmire, K. H. In *Comprehensive Organometallic Chemistry II*; Wilkinson, G., Stone, F. G. A., Abel, E., Eds.; Pergamon Press: New York, 1995; Vol. 7, Chapter 1, Section 1.11.2.2, p 62.

(3) (a) Adams, R. D. *Polyhedron* **1985**, *4*, 2003. (b) Adams, R. D.; Babin, J. E.; Mathur, P.; Natarajan, K.; Wang, J.-G. *Inorg. Chem.* **1989**, *28*, 1440. (c) Adams, R. D.; Wang, J.-G. *Polyhedron* **1989**, *8*, 1437. (d) Adams, R. D.; Babin, J. E.; Estrada, J.; Wang, J.-G.; Hall, M. B.; Low, A. A. *Polyhedron* **1989**, *8*, 1885. (e) Mathur, P.; Mukhopadhyay, S.; Ahmed, M. O.; Lahiri, G. K.; Chakraborty, S.; Walawalker, M. G. *Organometallics* **2000**, *19*, 5787. (f) Mathur, P.; Mukhopadhyay, S.; Lahiri, G. K.; Chakraborty, S.; Thöne, C. *Organometallics* **2002**, *21*, 5209. (g) Scheer, M.; Umbarkar, S. B.; Chatterjee, S.; Trivedi, R.; Mathur, P. *Angew. Chem., Int. Ed.* **2001**, *40*, 376.

(4) (a) Westmeyer, M. D.; Rauchfuss, T. B. *Inorg. Chem.* **1996**, *35*, 7140. (b) Westmeyer, M. D.; Galloway, C. P.; Rauchfuss, T. B. *Inorg. Chem.* **1994**, *33*, 4615. (c) Day, V. W.; Lesch, D. A.; Rauchfuss, T. B. *J. Am. Chem. Soc.* **1982**, *104*, 1290.

(5) (a) Cowie, M.; DeKock, R. L.; Wagenmaker, T. R.; Seyferth, D.; Henderson, R. S.; Gallagher, M. K. *Organometallics* **1989**, *8*, 119. (b) Song, L.-C.; Lu, G. L.; Hu, Q.-M.; Fan, H.-T.; Chen, Y.; Sun, J. *Organometallics* **1999**, *12*, 3258. (c) Song, L. C.; Kidiata, M.; Wang, J.-T.; Wang, R.-J.; Wang, H.-J. *J. Organomet. Chem.* **1990**, *391*, 397. (d) Bose, K. S.; Sinn, E.; Averill, B. A. *Organometallics* **1984**, *3*, 1126. (e) Don, M. J.; Yang, K. Y.; Bott, S. G.; Richmond, M. G. *J. Coord. Chem.* **1996**, *40*, 273.

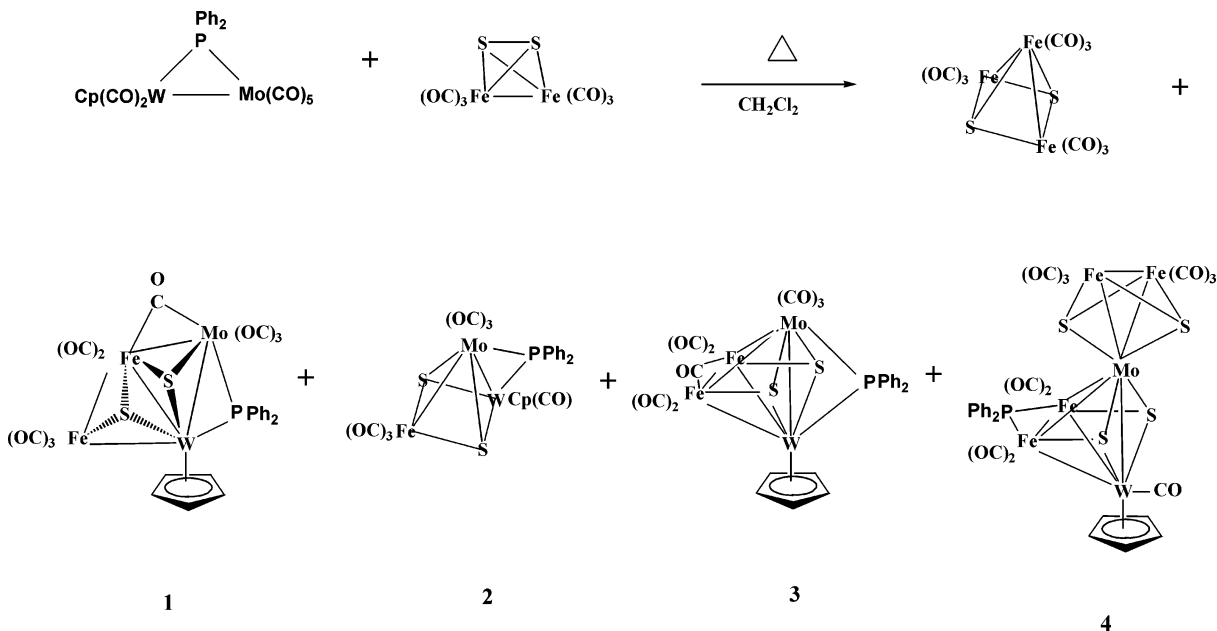
(6) King, R. B.; Bitterwolf, T. E. *Coord. Chem. Rev.* **2000**, *206–207*, 563.

(7) Song, L.-C.; Fan, H.-T.; Hu, Q.-M. *J. Am. Chem. Soc.* **2002**, *124*, 4566.

(8) (a) Seyferth, D.; Henderson, R. S. *J. Am. Chem. Soc.* **1979**, *101*, 508. (b) Seyferth, D.; Henderson, R. S.; Song, L.-C. *J. Organomet. Chem.* **1980**, *192*, C1.

(9) (a) Vahrenkamp, H.; Wucherer, E. J. *Angew. Chem., Int. Ed. Engl.* **1981**, *20*, 680. (b) Braunstein, P.; Jud, J.-M.; Tiripicchio, A.; Camellini, M. T.; Sappa, E. *Angew. Chem., Int. Ed. Engl.* **1982**, *21*, 307. (c) Braunstein, P.; Tiripicchio, A.; Camellini, M. T.; Sappa, E. *Inorg. Chem.* **1981**, *20*, 358. (d) Williams, P. D.; Curtis, M. D.; Duffy, D. N.; Butler, W. M. *Organometallics* **1983**, *2*, 165.

Scheme 1



reported. Here we report an insertion reaction between $\text{Fe}_2(\mu\text{-S}_2)(\text{CO})_6$ and the phosphido-bridged heterodinuclear $\text{CpW(CO)}_2(\mu\text{-PPh}_2)\text{Mo(CO)}_5$, which has a weak Mo–W bond and labile CO ligands on Mo for further reaction.¹⁰ This reaction leads to an unusual fragmentation and coordination of $\text{Fe}_2(\mu\text{-S}_2)(\text{CO})_6$, both of which, to our knowledge, are the first examples of such reactivity of the diiron complex. The substitution reactions on **3** by norbornadiene and benzene are also described.

Results and Discussion

Reaction of $\text{Fe}_2(\mu\text{-S}_2)(\text{CO})_6$ with $\text{CpW(CO)}_2(\mu\text{-PPh}_2)\text{Mo(CO)}_5$. When a dichloromethane solution of $\text{Fe}_2(\mu\text{-S}_2)(\text{CO})_6$ and $\text{CpW(CO)}_2(\mu\text{-PPh}_2)\text{Mo(CO)}_5$ was refluxed for about 20 h, clusters **1–4** and a known compound $\text{Fe}_3(\mu\text{-S})_2(\text{CO})_9$ were obtained (Scheme 1).

Control experiments established that $\text{Fe}_2(\mu\text{-S}_2)(\text{CO})_6$ alone did not convert to $\text{Fe}_3(\mu\text{-S})_2(\text{CO})_9$ and that $\text{Fe}_3(\mu\text{-S})_2(\text{CO})_9$ did not react with $\text{CpW(CO)}_2(\mu\text{-PPh}_2)\text{Mo(CO)}_5$ under identical conditions; therefore, they formed directly from $\text{Fe}_2(\mu\text{-S}_2)(\text{CO})_6$ and $\text{CpW(CO)}_2(\mu\text{-PPh}_2)\text{Mo(CO)}_5$.

Cluster **1** has a bitetrahedral geometry (Figure 1) with FeMoWS and Fe_2WS tetrahedra, where each S atom is coordinated to metals in a $\mu_3\text{-S}$ mode. The molecular structure of **2** (Figure 2) reveals a square pyramidal geometry, with the FeS_2W plane capped by a Mo atom. Each sulfur atom is coordinated to FeW Mo atoms in a $\mu_3\text{-S}$ mode. There are a few examples of heterobimetallic square pyramidal clusters with an $\text{Fe}_2\text{M}(\mu_3\text{-S})_2$ core (M = Co, W, Ru),¹¹ which were

obtained by insertion of coordinatively unsaturated metal species into the S–S bond of $\text{Fe}_2(\mu\text{-S}_2)(\text{CO})_6$. Cluster **2** is a rare example of a heterotrimetallic cluster

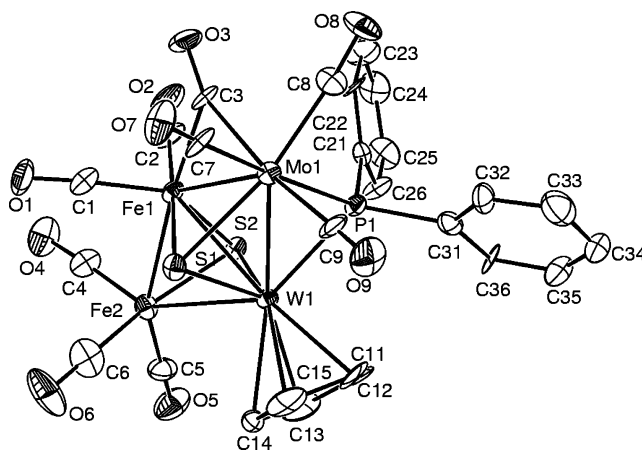


Figure 1. ORTEP drawing of **1**. Hydrogen atoms are omitted.

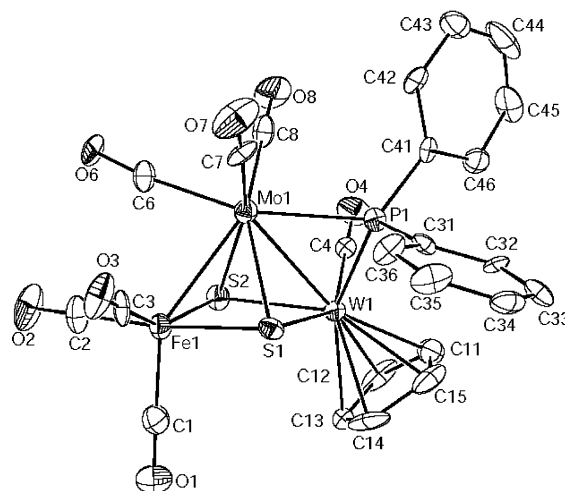


Figure 2. ORTEP drawing of **2**. Hydrogen atoms are omitted.

(10) Shyu, S.-G.; Hsu, J.-Y.; Lin, P.-J.; Wu, W.-J.; Peng, S.-M.; Lee, G.-H.; Wen, Y.-S. *Organometallics* **1994**, *13*, 1699.

(11) (a) Adams, R. D.; Babin, J. E.; Wang, J.-G.; Wu, W. *Inorg. Chem.* **1989**, *28*, 703. (b) Wakatsuki, Y.; Yamazaki, H.; Chen, G. *J. Organomet. Chem.* **1988**, *347*, 151. (c) Mathur, P.; Chakrabarty, D.; Mavunkal, I. *J. J. Cluster Sci.* **1993**, *4*, 351.

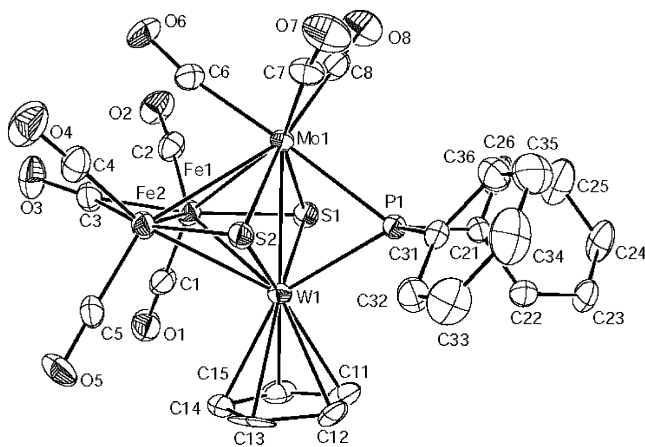


Figure 3. ORTEP drawing of **3**. Hydrogen atoms are omitted.

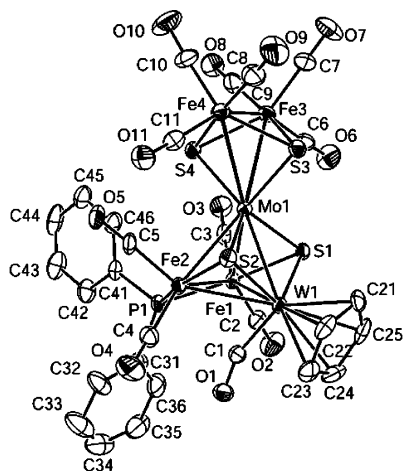


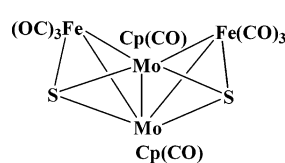
Figure 4. ORTEP drawing of **4**. Hydrogen atoms are omitted.

with square pyramidal geometry. There were no reports of square pyramidal heterotrimetallic clusters with bridging sulfur owing to a lack of availability of heterodinuclear building blocks such as $\text{MM}'(\mu\text{-S}_2)(\text{CO})_6$ except the recent reports of the $\text{CpMnCo}(\mu\text{-S}_2)(\text{CO})_5$.¹² The tetrametallic cluster **3** consists of an Fe_2MoW tetrahedron core with each FeMoW face capped by a $\mu_3\text{-S}$ atom. Its core structure (Figure 3) resembles more that of $\text{Cp}_2\text{Mo}_2\text{Fe}_2\text{S}_2(\text{CO})_7$ ¹³ and $\text{Cp}_2\text{Mo}_2\text{Fe}_2\text{Te}_2(\text{CO})_7$ ¹⁴ than that of $\text{Cp}_2\text{Mo}_2\text{Fe}_2\text{S}_2(\text{CO})_8$.^{9b,d}

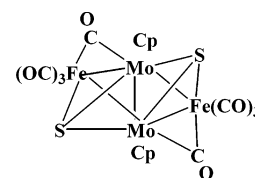
The novel hexametallic cluster **4** has a core structure (Figure 4) similar to that of **3**, but with the bridging ligands PPh_2 on MoW and CO on iron atoms having interchanged their positions. Ligand PPh_2 bridges the iron atoms, but CO is coordinated to tungsten as a terminal ligand. Moreover, the carbonyl ligands on Mo were replaced by another molecule of $\text{Fe}_2(\mu\text{-S}_2)(\text{CO})_6$. The coordination of this molecule to Mo is unique and unusual; it occupies four coordination sites on Mo by using all the Fe_2S_2 atoms. The resulting geometry of $\text{Fe}_2\text{S}_2\text{Mo}$ is that of a trigonal bipyramid, with the $\text{Fe}_2\text{-}$

Mo triangle attached to two apical $\mu_3\text{-S}$. This arrangement provides striking contrast with the generally observed square planar geometry in $\text{WFe}_2(\text{CO})_9(\text{PMe}_2\text{-Ph})(\mu_3\text{-S})_2$,^{11a} $(\text{C}_5\text{H}_4\text{COOMe})\text{CoFe}_2(\text{CO})_2(\mu_3\text{-S})_2$,^{11b} $\text{Cp}^*\text{Co}(\mu_3\text{-S})_2\text{Fe}_2(\text{CO})_6$,^{5a} and $\text{Fe}_2\text{Ru}(\mu_3\text{-S})_2(\text{CO})_9$.^{11c}

Formation of Clusters 1 and 2: Role of the Phosphido Bridge. It has been reported that during the reaction between $\text{Fe}_3(\mu\text{-Te})_2(\text{CO})_9$ and dinuclear $\text{Cp}_2\text{Mo}_2(\text{CO})_6$, $\text{Fe}_3(\mu\text{-Te})_2(\text{CO})_9$ converted to more reactive $\text{Fe}_2(\mu\text{-Te}_2)(\text{CO})_6$, which further reacted with $\text{Cp}_2\text{Mo}_2(\text{CO})_6$ to form a five-vertex, arachno cluster, $\text{Cp}_2\text{Mo}_2\text{FeTe}_2(\text{CO})_7$.¹⁴ Rauchfuss proposed that the formation of $\text{Cp}_2\text{Mo}_2\text{FeTe}_2(\text{CO})_7$ was possibly by the loss of an even-electron $\text{Fe}(\text{CO})_n$ fragment from either octahedral or bitetrahedral $\text{Mo}_2\text{Fe}_2\text{Te}_2$ clusters.¹⁴ However, during the reaction of $\text{Fe}_2(\mu\text{-S}_2)(\text{CO})_6$ or $\text{Fe}_3(\mu\text{-S})_2(\text{CO})_9$ with $\text{Cp}_2\text{Mo}_2(\text{CO})_6$ in identical conditions, the cis isomer (Braunstein isomer), $\text{Cp}_2\text{Mo}_2\text{Fe}_2\text{S}_2(\text{CO})_8$, was observed instead of $\text{Cp}_2\text{Mo}_2\text{FeS}_2(\text{CO})_7$, the analogue of $\text{Cp}_2\text{Mo}_2\text{FeTe}_2(\text{CO})_7$.¹⁴ Rauchfuss also reported that under the conditions of his experiment, the expected trans isomer (Curtis isomer) is converted into the cis form. The cis and trans isomers of $\text{Cp}_2\text{Mo}_2\text{Fe}_2\text{S}_2(\text{CO})_8$ were obtained from $\text{Cp}_2\text{Mo}_2(\text{CO})_4$ and $\text{Fe}_2(\mu\text{-S}_2)(\text{CO})_6$.^{9b,d}



Braunstein isomer



Curtis isomer

The Braunstein isomer of $\text{Cp}_2\text{Mo}_2\text{Fe}_2\text{S}_2(\text{CO})_8$ resembles in structure that of $\text{Cp}_2\text{Mo}_2\text{Fe}_2\text{Te}_2(\text{CO})_7$, which is a thermolytic product of $\text{Cp}_2\text{Mo}_2\text{FeTe}_2(\text{CO})_7$. He then proposed that formation of the Braunstein–Curtis isomers may also occur via a Mo_2FeS_2 ¹⁴ intermediate similar to Mo_2FeTe_2 ,¹⁴ but it is unstable compared to Mo_2FeTe_2 .¹⁴ Here we observed the MoWFeS_2 core cluster **2**, when $\text{Fe}_2(\mu\text{-S}_2)(\text{CO})_6$ reacted with the heterodinuclear phosphido-bridged $\text{CpW}(\text{CO})_2(\mu\text{-PPh}_2)\text{Mo}(\text{CO})_5$. It has a five-vertex *nido* structure rather than a five-vertex *arachno* geometry like $\text{Cp}_2\text{Mo}_2\text{FeTe}_2(\text{CO})_7$.

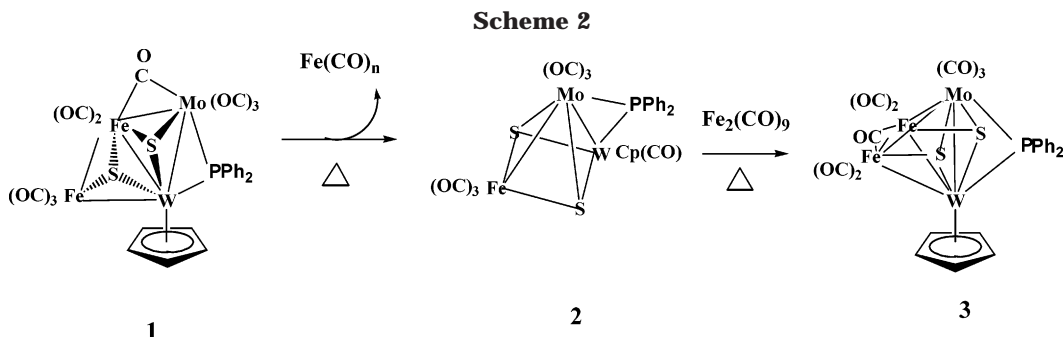
The bridged phosphido ligand in $\text{CpW}(\text{CO})_2(\mu\text{-PPh}_2)\text{Mo}(\text{CO})_5$ may prevent the cleavage of the Mo–W bond during the reaction and lead to a stable **2** with a *nido* structure. We also isolated bitetrahedral **1**, which is an analogue of the proposed bitetrahedral $\text{Mo}_2\text{Fe}_2\text{Te}_2$ ¹⁴ intermediate in the reaction between $\text{Fe}_3(\mu\text{-Te})_2(\text{CO})_9$ and $\text{Cp}_2\text{Mo}_2(\text{CO})_6$. Stability in **1** may also be caused by the bridged phosphido ligand.

Mechanism of the Formation of 3. When a dichloromethane solution of **1** was refluxed for 20 h, **3** was the sole product. It is realized that **1** is rearranged to **3** after loss of one carbonyl ligand compensated for by formation of an Fe–Mo bond, and the bridging carbonyl shifted from the Fe–Mo to Fe–Fe position with breaking an Fe–S bond and making a Mo–S bond. On the other hand **2** differs from **1** and **3** by an $\text{Fe}(\text{CO})_n$ fragment (Scheme 2). Thus, this rearrangement of **1** to **3** may occur via **2** by dissociation–reassociation of $\text{Fe}(\text{CO})_n$. It is further supported by the conversion of **2** to **3** with $\text{Fe}_2(\text{CO})_9$. We did not observe **2**, as an

(12) (a) Adams, R. D., Miao, S. *Organometallics* **2003**, *22*, 2492. (b) Adams, R. D.; Captain, B.; Kwon, O.-S.; Miao, S. *Inorg. Chem.* **2003**, *22*, 3356.

(13) Mathur, P.; Hossain, Md. M.; Rheingold, A. L. *Organometallics* **1994**, *13*, 3909.

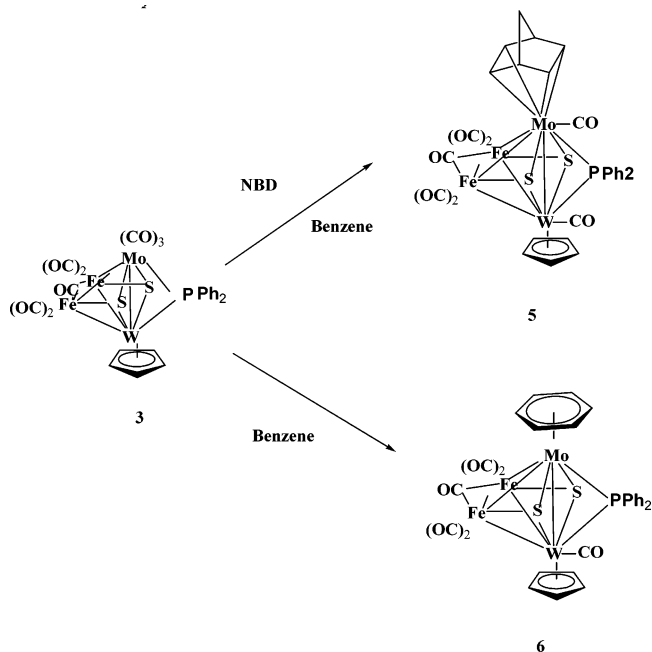
(14) Bogan, L. E., Jr.; Rauchfuss, T. B.; Rheingold, A. L. *J. Am. Chem. Soc.* **1985**, *107*, 3843.



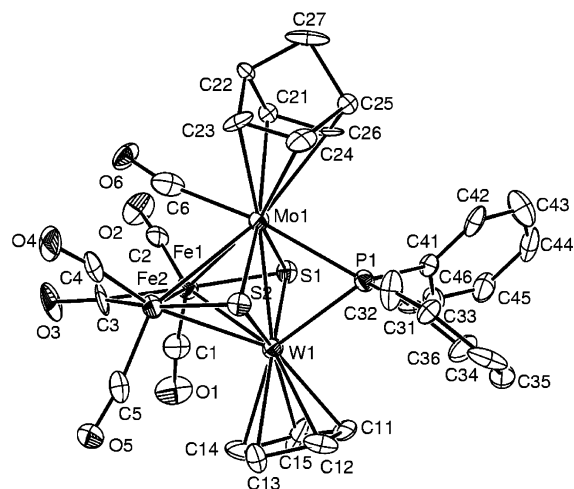
intermediate during thermolysis of **1** to **3** may be due to two reasons. First, the dissociation–reassociation of $\text{Fe}(\text{CO})_n$ is spontaneous and stoichiometric. Second there was no acceptor of $\text{Fe}(\text{CO})_n$ other than the dissociated product **2** in the reaction medium. However, we isolated **2** during reaction between $\text{Fe}_2(\mu\text{-S}_2)(\text{CO})_6$ and $\text{CpW}(\text{CO})_2(\mu\text{-PPh}_2)\text{Mo}(\text{CO})_5$. This is because some of the dissociated $\text{Fe}(\text{CO})_n$ from **1** also reacted with $\text{Fe}_2(\mu\text{-S}_2)(\text{CO})_6$ and formed $\text{Fe}_3(\mu\text{-S}_2)(\text{CO})_9$ leaving some of **2** intact. This is further supported by the formation of $\text{Fe}_3(\mu\text{-S}_2)(\text{CO})_9$ and **2** together with **3**, when **1** was thermolyzed in identical conditions in the presence of $\text{Fe}_2(\mu\text{-S}_2)(\text{CO})_6$. In support of this fragmentation mechanism, we could mention the reversible dissociation of an $\text{Fe}(\text{CO})_3$ vertex of $\text{Fe}_4(\text{PPh}_2)(\text{CO})_{12}$ to produce $\text{Fe}_3(\text{PPh}_2)(\text{CO})_9$.¹⁵ Formation of intermediates **1** and **2** for **3** also supports Rauchfuss' proposal about the intermediates bitetrahedral $\text{Mo}_2\text{Fe}_2\text{Te}_2$ ¹⁴ and Mo_2FeS_2 ¹⁴ for the reactions of $\text{Fe}_3(\mu\text{-Te})_2(\text{CO})_9$ with $\text{Cp}_2\text{Mo}_2(\text{CO})_6$ and $\text{Fe}_2(\mu\text{-S}_2)(\text{CO})_x$ ($x = 6, 9$) with $\text{Cp}_2\text{Mo}_2(\text{CO})_x$ ($x = 4, 6$),^{9b,d,14} respectively.

Reaction of 3 with Norbornadiene (nbd), Benzene, and $\text{Fe}_2(\mu\text{-S}_2)(\text{CO})_6$. When a benzene solution of **3** is refluxed with nbd, cluster **5** is an isolated product, but the same reaction without nbd afforded cluster **6** (Scheme 3). The core Fe_2MoW of **5** and **6** has a geometry (Figures 5 and 6) similar to that of **3**. Basically both of them are substitution products of **3** where carbonyl ligands on Mo are replaced by nbd and C_6H_6 , respectively. This indicates that carbonyl ligands on the Mo site are more labile than those on Fe sites. Carbonyl ligands are π acceptors. Due to the high oxidation state of the Mo atom in **3**, the availability of electron density on it for back-donation to carbonyl ligands is reduced; therefore the Mo–C bond is weakened and becomes more labile for substitution. Formation of **4** was expected from the reaction between **3** and $\text{Fe}_2(\mu\text{-S}_2)(\text{CO})_6$. However, a control reaction of **3** with $\text{Fe}_2(\mu\text{-S}_2)(\text{CO})_6$ did not produce **4**.

X-ray Structures of Clusters 1–6. Molecular structures of **1–6** were determined by single-crystal X-ray diffraction analyses, and they are shown in Figures 1–6, respectively. The experimental data are summarized in Table 1. Selected bond distances and bond angles are listed in Table 2. Cluster **1** contains 62 valence electrons assuming each sulfur atom serves as a four-electron donor. To obey the 18e rule, tetrametallic **1** possesses five metal–metal bonds. Thus, the square Fe1Fe2Mo1W1

Scheme 3

in **1** is intercepted by a fifth diagonal Fe1–W1 bond, resulting in bitetrahedral Fe1Fe2W1S2 and Fe1Mo1W1S1 . Overall, the structure of **1** is similar to $\text{WFe}_3(\text{CO})_{11}(\text{PMe}_2\text{Ph})(\mu_3\text{-S})_2$.^{11a} The peripheral Fe–W bonds in these two clusters are comparable; however, the diagonal Fe1–W1 (2.7516(19) Å) in **1** is longer than the diagonal Fe2–W (2.667(1) Å) in $\text{WFe}_3(\text{CO})_{11}(\text{PMe}_2\text{Ph})(\mu_3\text{-S})_2$. Cluster **2** consists of 50 valence electrons,

**Figure 5.** ORTEP drawing of **5**. Hydrogen atoms are omitted.

(15) (a) Vahrenkamp, H.; Wolters, D. *J. Organomet. Chem.* **1982**, *224*, C17. (b) Vahrenkamp, H.; Wucherer, E. J.; Wolters, D. *Chem. Ber.* **1983**, *116*, 1219.

Table 1. Summary of Crystal Data for 1–3 and 4–6

	1	2	3
formula	$C_{26}H_{15}O_9Fe_2PS_2MoW$	$C_{24}H_{15}O_7S_2PFeMoW$	$C_{25}H_{15}O_8S_2PFe_2MoW$
fw	957.96	846.1	929.95
space group	$P21/n$	$P1211$	$P121/c1$
a [Å]	9.6344(17)	8.943(3)	9.9693(15)
b [Å]	24.805(4)	9.702(2)	14.942(2)
c [Å]	12.414(2)	15.436(3)	19.291(3)
α [deg]			
β [deg]	92.318(15)	96.58(2)	91.221(13)
γ [deg]			
V [Å ³]	2964.3(9)	1330.5(6)	2872.9(8)
ρ (calcd) [Mg m ⁻³]	2.147	2.112	2.150
Z	4	1	4
cryst dimens [mm]	$0.25 \times 0.20 \times 0.14$	$0.24 \times 0.20 \times 0.14$	$0.24 \times 0.12 \times 0.09$
temp	room temperature	room temperature	room temperature
λ (Mo K α) [Å]	0.71073	0.71073	0.71073
2θ range [deg]	50	50.0	50.0
scan type	ω	ω	ω
no. of reflns	5525	2687	5338
no. of obsd reflns	5200 ($>2.0\sigma(I)$)	2517 ($>2.5\sigma(I)$)	5034 ($>2.0\sigma(I)$)
no. of params refined	380	339	421
R	0.0395	0.0526	0.0257
R_w	0.1040	0.1263	0.0558
GoF	1.065	1.019	1.043
D_{map} min., max. [e/Å ³]	-1.762, 1.598	-2.379, 2.828	-0.463, 0.482

	4	5	6
formula	$C_{29}H_{17}O_{11}PS_4Cl_2Fe_4MoW$	$C_{30}H_{23}O_6S_2PFe_2MoW$	$C_{42}H_{37}O_5S_2PFe_2MoW$
fw	1274.76	966.08	1108.32
space group	$P21/n$	$P121/c1$	$P121/n1$
a [Å]	10.2336(14)	10.5679(13)	10.400(2)
b [Å]	16.749(3)	19.380(3)	19.407(4)
c [Å]	23.139(4)	15.794(3)	20.383(4)
α [deg]			
β [deg]	102.486(14)	93.652(13)	91.41(3)
γ [deg]			
V [Å ³]	3872.3(11)	3228.1(10)	4112.5(14)
ρ (calcd) [Mg m ⁻³]	2.183	1.979	1.790
Z	4	4	6
cryst dimens [mm]	$0.25 \times 0.10 \times 0.06$	$0.19 \times 0.17 \times 0.07$	$0.44 \times 0.38 \times 0.28$
temp	room temperature	room temperature	room temperature
λ (Mo K α) [Å]	0.71073	0.71073	0.71073
2θ range [deg]	50.0	50.0	50.0
scan type	ω	ω	ω
no. of reflns	7203	5666	7665
no. of obsd reflns	6784 ($>2.0\sigma(I)$)	5448 ($>2.0\sigma(I)$)	7235 ($>2.0\sigma(I)$)
no. of params refined	519	371	487
R	0.038	0.0667	0.0317
R_w	0.096	0.1850	0.0783
GoF	1.059	0.966	1.056
D_{map} min., max. [e/Å ³]	-1.669, 1.786	-1.216, 5.197	-0.838, 0.850

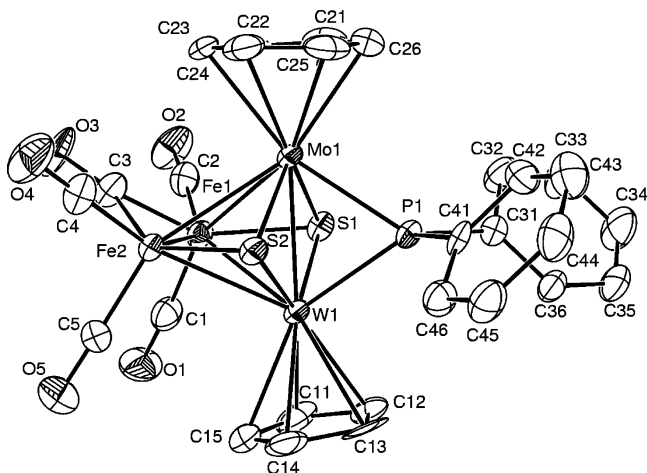


Figure 6. ORTEP drawing of **6**. Hydrogen atoms are omitted.

which satisfies the 18e rule, providing a trinuclear two metal–metal bonded square pyramidal geometry. The

number of electrons expected for a normal trinuclear triangle cluster is 48; the excess two electrons in **2** cleaved one metal–metal bond and formed square pyramidal **2**. It is structurally similar to $WFe_2(CO)_9-(PMe_2Ph)(\mu_3-S)_2$,^{11a} $(C_5H_4COOMe)CoFe_2(CO)_2(\mu_3-S)_2$,^{11b} and $Fe_2Ru(\mu_3-S)_2(CO)_9$.^{11c} Cluster **3** is electron precise with 60 valence electrons. Thus, the tetranuclear **3** has six metal–metal bonds to satisfy 18e for each metal. It has two electrons less than **1** (62e) after loss of one CO compensated for by an extra metal–metal bond. Both **5** and **6** are also electron precise, with 60 valence electrons, similar to that of **3**, where two CO for **5** and three CO for **6** on the Mo site were substituted by a four-electron donor nbd and a six-electron donor benzene, respectively. Therefore, they are also structurally very similar to **3**. In comparison with the Braunstein isomer of $Cp_2Mo_2Fe_2S_2(CO)_8$, clusters **3**, **5**, and **6** have an Fe–Fe bond bridged by CO instead of any semitriply bridged CO, both of those being seen on Mo atoms in $Cp_2Mo_2Fe_2S_2(CO)_8$.^{9b,d} The Fe–Fe bond lengths in **3**

Table 2. Selected Bond Lengths (Å) and Bond Angles (deg) for 1–6

	1	2	3	4	5	6
			Bonds			
Mo1–W1	2.9155(13)	2.865(3)	2.7196(6)	2.8172(9)	2.698(3)	2.6732(6)
Mo1–Fe1	2.814(2)	2.753(4)	2.8445(9)	2.7622(16)	2.830(4)	2.8304(12)
Mo1–Fe2			2.8374(9)	2.7555(15)	2.879(4)	2.8181(12)
Mo1–Fe3				2.8919(16)		
Mo1–Fe4				2.8967(17)		
W1–Fe1	2.7516(19)		2.7595(8)	2.7724(14)	2.758(4)	2.7335(9)
W1–Fe2	2.834(2)		2.7659(8)	2.7819(14)	2.768(4)	2.7627(9)
Fe1–Fe2	2.592(3)		2.4192(10)	2.5673(19)	2.517(6)	2.4226(12)
Fe3–Fe4				2.527(2)		
Mo1–S1	2.448(4)	2.475(7)	2.4887(13)	2.321(2)	2.443(7)	2.4146(16)
Mo1–S2		2.503(7)	2.4668(13)	2.320(2)	2.501(7)	2.4088(15)
Mo1–S3				2.308(3)		
Mo1–S4				2.299(3)		
W1–S1	2.298(3)	2.484(5)	2.3315(13)	2.321(2)	2.450(7)	2.3416(14)
W1–S2	2.295(3)	2.420(9)	2.3268(12)	2.321(2)	2.376(6)	2.3410(14)
Fe1–S1	2.281(4)	2.258(8)	2.1738(15)	2.238(3)	2.219(7)	2.1760(17)
Fe1–S2	2.290(4)	2.251(7)				
Fe2–S2	2.154(4)		2.1751(14)	2.244(3)	2.204(7)	2.1749(16)
Fe3–S3				2.298(3)		
F3–S4				2.289(3)		
Fe4–S3				2.281(3)		
Fe4–S4				2.298(3)		
Mo1–P1	2.461(3)	2.496(7)	2.5186(13)		2.549(7)	2.4359(14)
W1–P1	2.438(4)	2.403(5)	2.4580(13)		2.452(6)	2.4117(16)
Fe1–P1				2.191(3)		
Fe2–P1				2.202(3)		
Fe1–C1	1.733(16)	1.79(3)	1.750(6)		1.64(3)	1.734(8)
Fe1–C2	1.763(15)	1.83(3)	1.782(6)		1.87(3)	1.775(7)
Fe1–C3	2.121(16)	1.80(2)	1.956(6)		2.00(3)	1.923(60)
Fe2–C3			1.947(6)		1.94(3)	1.924(6)
Fe2–C4	1.746(17)		1.757(6)		1.72(3)	1.773(6)
Fe2–C5	1.759(17)		1.793(6)		1.78(3)	1.748(7)
			Angles			
S1–W1–S2	102.90(12)	74.3(2)	116.12(4)	104.12(5)	115.0(2)	113.92(5)
S1–W1–P1	107.85(12)	74.12(17)	75.64(4)		73.2(2)	74.52(6)
S1–W1–Mo1	54.47(9)	54.57(18)	58.43(3)	52.63(3)	56.42(17)	57.11(4)
S1–W1–Fe1	52.79(9)		49.69(4)	51.19(6)	50.01(17)	50.05(4)
S1–W1–Fe2	74.49(10)		95.52(4)	95.89(6)	97.19(18)	95.27(4)
S2–W1–P1	83.27(12)	111.0(3)	75.96(4)		76.8(2)	74.44(6)
S2–W1–Mo1	101.02(9)	55.78(19)	57.90(3)	52.61(6)	58.65(17)	56.96(4)
S2–W1–Fe1	53.03(9)		95.49(3)	96.17(7)	97.28(8)	95.50(4)
S2–W1–Fe2	48.28(9)		49.65(3)	51.20(7)	50.05(17)	49.61(4)
P1–W1–Mo1	53.85(8)	55.75(18)	57.95(3)		59.10(18)	56.97(3)
P1–W1–Fe1	84.74(9)		113.96(4)		114.09(19)	113.8(4)
P1–W1–Fe2	128.81(9)		114.13(3)		116.14(19)	113.11(4)
Mo1–W1–Fe1	59.46(9)		62.55(2)	59.22(3)	62.49(9)	63.12(3)
Mo1–W1–Fe2	112.85(5)		62.29(2)	58.96(3)	63.57(9)	62.43(3)
Fe1–W1–Fe2	55.27(6)		51.93(2)	55.06(5)	54.19(12)	52.30(3)
S1–Mo1–S2		73.0(2)	105.82(4)	104.69(9)	110.8(2)	108.93(5)
S1–Mo1–P1	102.50(12)	72.7(2)	71.86(14)		71.6(2)	72.79(5)
S1–Mo1–W1	49.81(8)	54.85(14)	52.96(3)	52.63(6)	56.66(16)	54.51(4)
S1–Mo1–Fe1	50.80(9)	50.82(17)	47.53(3)	51.35(7)	49.09(17)	48.22(4)
S1–Mo1–Fe2			90.33(4)	96.60(7)	94.48(9)	92.23(5)
S2–Mo1–P1		105.3(2)	72.45(4)		72.9(2)	72.81(5)
S2–Mo1–W1		53.08(19)	53.04(3)	52.65(6)	54.23(16)	54.56(4)
S2–Mo1–Fe1		50.44	90.33(4)	96.48(7)	92.62(18)	91.54(4)
S2–Mo1–Fe2			47.79(3)	51.61(7)	47.74(17)	48.40(4)
P1–Mo1–W1	53.12(9)	52.71(14)	55.81(3)		55.64(15)	56.10(4)
P1–Mo1–Fe1	82.99(9)	121.78(18)	109.28(4)		108.72(18)	109.78(4)
P1–Mo1–Fe2			109.86(7)		109.36(18)	110.48(4)
W1–Mo1–Fe1	57.37(4)	80.86(9)	59.41(2)	59.58(3)	59.80(9)	59.48(2)
W1–Mo1–Fe2			59.66(2)	59.88(3)	59.40(10)	60.34(2)
Fe1–Mo1–Fe2			50.40(2)	55.46(4)	52.30(12)	50.79(3)
S1–Fe1–Fe2	79.81(11)		110.88(4)	104.36(8)	111.5(2)	110.53(6)
S1–Fe1–W1	53.35(9)		54.86(4)	53.91(7)	57.8(2)	55.57(4)
S1–Fe1–Mo1	56.27(10)	58.20(17)	57.62(4)	54.08(7)	56.31(19)	55.85(4)
Fe2–Fe1–W1	63.98(6)		64.17(3)	62.66(4)	63.10(12)	64.47(3)
Fe2–Fe1–Mo1	124.73(8)		64.65(3)	62.14(5)	64.85(13)	64.34(4)
W1–Fe1–Mo1	63.17(5)		58.0541(15)	61.19(3)	57.71(9)	57.40(2)
S2–Fe1–Mo1	104.22(10)	59.0(2)				
S2–Fe2–Fe1	56.79(10)		110.43(5)	104.23(8)	109.6(2)	109.85(5)
S2–Fe2–W1	52.67(9)		54.61(4)	53.73(7)	55.70(19)	55.06(4)
S2–Fe2–Mo1			57.14(4)	54.14(7)	57.03(9)	55.92(4)
Fe1–Fe2–W1	60.75(6)		63.90(3)	62.28(4)	62.71(13)	63.23(3)

Table 2 (Continued)

	1	2	3	4	5	6
Fe1–Fe2–Mo1			64.95(3)	62.40(4)	63.86(13)	64.87(4)
W1–Fe2–Mo1			58.056(19)	61.16(3)	57.03(9)	57.23(2)
Fe1–S1–W1	73.87(10)	100.3(3)	75.45(5)	74.90(8)	72.2(2)	74.38(5)
Fe1–S1–Mo1	72.93(11)	71.0(2)	74.85(4)	74.57(8)	74.6(2)	75.93(5)
Fe1–S2–W1	73.76(10)	70.6(2)				
Fe1–S2–Mo1		102.5(3)				
Fe2–S2–W1	79.05(11)		75.73(4)	75.06(8)	74.2(2)	75.33(5)
Fe2–S2–Mo1			75.08(5)	74.25(8)	75.2(2)	75.68(5)
W1–S1–Mo1	75.73(10)	70.58(17)	68.61(3)	74.75(7)	66.92(19)	68.38(4)
W1–S2–Mo1		71.1(2)	69.06(4)	74.73(7)	67.12(17)	68.48(4)
W1–P1–Mo1	73.03(10)	71.54(18)	66.24(3)		65.26(17)	66.93(4)
Fe2–C3–Fe1			76.6(2)		79.2(10)	78.1(2)

Table 3. Bond Distances for a Few Bridged Binuclear Molybdenum and Tungsten Complexes

compound	bridge no.	M–M (Å)	M–X–M (deg)	ref
$\text{Cp}(\text{CO})_2\text{W}(\mu\text{-PPh}_2)\text{W}(\text{CO})_5$	1	3.1942(12)	81.02(18)	20
$\text{Cp}(\text{CO})_2\text{W}(\mu\text{-PPh}_2)\text{Mo}(\text{CO})_5$	1	3.2054(16)	81.31(14)	10
$\text{Cp}(\text{CO})_2\text{Mo}(\mu\text{-SMe})\text{W}(\text{CO})_5$	1	3.131(1)	79.49(1)	21
$(\text{CO})_4\text{W}(\mu\text{-SPh})_2\text{W}(\text{CO})_4$	2	2.972(1)		22
$\text{Cp}(\text{CO})_2\text{W}(\mu\text{-SMe})(\mu\text{-I})\text{W}(\text{CO})_3\text{I}$	2	2.936(1)	73.2(1)	23
$\text{CpW}(\text{CO})(\mu\text{-SPh})_2(\mu\text{-PPh}_2)\text{Mo}(\text{CO})(\text{SPh})_2$	3	2.8589(6)	70.12(av)	24
$\text{CpW}(\text{CO})(\mu\text{-SPh})_2(\mu\text{-PPh}_2)\text{Mo}(\text{CO})_3$	3	2.8427(14)	69.35(av)	24
$\text{CpW}(\text{CO})(\mu\text{-SPh})_2(\mu\text{-PPh}_2)\text{Mo}(\text{CO})_2(\text{PPh}_3)$	3	2.8382(13)	69.44(av)	24
$\text{CpW}(\text{CO})(\mu\text{-SPh})_2(\mu\text{-PPh}_2)\text{Mo}(\text{CO})_2(\text{PPh}_2\text{H})$	3	2.8063(20)	68.68(av)	24
$\text{Cp}(\text{CO})\text{Mo}(\mu\text{-SPh})_3\text{Mo}(\text{CO})\text{Cp}$	3	2.8040(9)	68.8(av)	25
$\text{Cp}(\text{CO})\text{Mo}(\mu\text{-SCH}_2\text{Ph})_3\text{Mo}(\text{CO})(\text{SCH}_2\text{Ph})_2$	3	2.779(4)	68.0(av)	25
$\text{Cp}(\text{CO})\text{Mo}(\mu\text{-SMe})_2(\mu\text{-SH})\text{Mo}(\text{CO})\text{Cp}(\text{BF}_4)$	3	2.772(2)	68.60(av)	26
$(\text{MePh})\text{Mo}(\mu\text{-SMe})_4\text{Mo}(\text{MePh})(\text{PF}_6)_2$	4	2.614(1)	64.33(av)	27
$\text{CpMo}(\mu\text{-SMe})_4\text{MoCp}$	4	2.603(2)	63.7(av)	28

(2.4192(10) Å) and **6** (2.4226(12) Å) are shorter than those in **1** (2.592(3) Å), **4** (2.542 (av) Å), **5** (2.517(6) Å), and $\text{Fe}_3\text{E}_2(\text{CO})_9$ (E = S (2.600 (av) Å),¹⁶ Se (2.650 Å (av)),¹⁶ but close to the very strong Fe–Fe bond (2.402 Å) in $(\text{NH}_2)_2\text{Fe}_2(\text{CO})_6$.¹⁷ Those bonds are even shorter than the carbonyl-bridged iron–iron bonds in $\text{Fe}_4(\text{PPh})(\text{CO})_{11}$ (2.440(3) Å),¹⁵ $\text{Cp}_2\text{Mo}_2\text{Fe}_2\text{Se}_2(\text{CO})_7$ (2.442(2) Å),¹³ and $\text{Cp}_2\text{Mo}_2\text{Fe}_2\text{Te}_2(\text{CO})_7$ (2.433(2) Å).¹⁴ Overall, they are only 0.0932 Å for **3** and 0.0966 Å for **6** longer than the formal double bond in $\text{Cp}_2\text{Fe}_2(\text{NO})_2$ (2.326(4) Å).¹⁸ The hexanuclear **4** with eight metal–metal bonds contains 90 valence electrons, which is two electron less to satisfy 18e for each metal atom. Thus, it is an electronically poor cluster. This shortening may force the $\text{Fe}_2(\mu\text{-S}_2)(\text{CO})_6$ to use all four of its atoms for coordination to the Mo atom to form two Mo–Fe bonds. Moreover, the average bond distance of Mo–S in **4** (2.312 Å) is shorter than that in **1** (2.448(4) Å), **2** (2.489 Å), **3** (2.478 Å), **5** (2.472 Å), and **6** (2.4112 Å) and that in $\text{Cp}^*(\text{CO})_2\text{W}(\mu\text{-CCPh})\text{MoFe}_4(\mu_3\text{-S})_3(\mu_4\text{-S})(\text{CO})_{12}$ (2.415 Å),^{3f} $[\text{Cp}^*\text{Mo}_3(\mu\text{-O})_2(\mu\text{-S})(\mu_3\text{-CCPh})\{\text{Fe}_2(\mu_3\text{-S})_2(\text{CO})_6\}_2]$ (2.401 Å),^{3f} $[\text{Cp}^*\text{WMo}_2(\mu\text{-O})_2(\mu\text{-S})(\mu_3\text{-CCPh})\{\text{Fe}_2(\mu_3\text{-S})_2(\text{CO})_6\}_2]$ (2.3794 Å),^{3f} and $\text{Cp}^*\text{WMo}(\text{O})_2(\mu\text{-O})(\mu\text{-CCPh})\text{Fe}_2(\mu_3\text{-S})_2(\text{CO})_6$ (2.434 Å),^{3f} where coordination modes of $\text{Fe}_2(\mu\text{-S}_2)(\text{CO})_6$ molecules to the Mo atom are almost the same as that in **4**. Such short Mo–S bonds in **4** indicate the existence of sulfur to molybdenum π -bonding,¹⁹ which may compensate for the decrease of electrons in **4**.

The Mo–W bond lengths with average values of the acute angles (M–X–M, X = S, P) are 2.9155(13) Å

(74.36°), 2.865(3) Å (71.07°), 2.7197(7) Å (67.98°), 2.8172(9) Å (74.74°), 2.698(3) Å (66.65°), and 2.6732(6) Å (67.93°) for **1–6**, respectively. The Mo–W bond lengths are shorter by 0.424 Å (av) compared to the W–Mo (3.2054(16) Å) bond length in the parent com-

pound $\text{Cp}(\text{CO})_2\text{W}(\mu\text{-PPh}_2)\text{Mo}(\text{CO})_5$.¹⁰ Table 3 compares known molybdenum and tungsten dimers involving single, double, triple, or quadruple bridges.^{20–28} It indicates that the metal–metal bond distances in dinuclear compounds vary depending on the number of bridging ligands between the metal atoms, becoming shorter when the number of bridging ligands increases. Therefore, the shortening of the Mo–W bond distance in clusters **1–6** is expected since the number of bridges in them are increased compared to that of the parent compound $\text{Cp}(\text{CO})_2\text{W}(\mu\text{-PPh}_2)\text{Mo}(\text{CO})_5$. Furthermore, the Mo–W lengths in doubly bridged **1** are longer than triply bridged **2**, **3**, **5**, and **6**. Moreover, the variation of the Mo–W lengths among them is in accord with their average values of the angles (M–X–M, X = S, P) in **1–6**, and those average values of the acute angles compare well with the reported values for the structures where

(20) Shyu, S.-G.; Wu, W.-J.; Wen, Y.-S.; Peng, S.-M.; Lee, G.-H. *J. Organomet. Chem.* **1995**, *489*, 113.

(21) Guerschais, J. E.; LeQuéré, J. L.; Pétillon, F. Y. Monojlovic-Muir, Lj.; Muir, K. W.; Sharp, D. W. A. *J. Chem. Soc., Dalton Trans.* **1982**, 283.

(22) Lucas, C. R.; Newlands, M. J.; Gabe, E. J.; Lee, F. L. *Can. J. Chem.* **1987**, *65*, 898.

(23) LeQuéré, J. L.; Pétillon, F. Y. Guerschais, J. E.; Monojlovic-Muir, Lj.; Muir, K. W.; Sharp, D. W. A. *J. Organomet. Chem.* **1983**, *249*, 127.

(24) Hossain, Md. M.; Lin, H.-M.; Shyu, S.-G. *Organometallics* **2003**, *22*, 3262.

(25) Dickson, R. S.; Fallon, G. D.; Jackson, W. R.; Polas, A. J. *Organomet. Chem.* **2000**, *607*, 156.

(26) Schollhammer, P.; Pétillon, F. Y.; Pichon, R.; Poder-Guillou, S.; Muir, K. W.; Monojlovic-Muir, Lj. *Organometallics* **1995**, *14*, 2277.

(27) Silverthorn, W. E.; Couldwell, C.; Prout, K. *J. Chem. Soc., Chem. Commun.* **1978**, 1009.

(28) Connolly, N. G.; Dahl, L. F. *J. Am. Chem. Soc.* **1970**, *92*, 7470.

(16) Wei, C. H.; Dahl, L. F. *Inorg. Chem.* **1965**, *4*, 493.

(17) Dahl, L. F.; Costello, W. R.; King, R. B. *J. Am. Chem. Soc.* **1968**, *90*, 5422.

(18) Claderon, J. L.; Fontana, S.; Frauendorfer, E.; Day, V. W.; Iske, S. D. A. *J. Organomet. Chem.* **1974**, *64*, C16.

(19) Chisholm, M. H.; Cornig, J. F.; Huffman, J. C. *Inorg. Chem.* **1984**, *23*, 754.

Table 4. Bond Distances for a Few Sulfur Clusters

cluster	Mo–Fe/W–Fe	Mo–S/W–S	Fe–S	Fe–Fe	ref
<i>cis</i> -Cp ₂ Fe ₂ Mo ₂ S ₂ (CO) ₈	2.816(av)	2.331(av)	2.165(8)		9b
<i>trans</i> -Cp* ₂ Fe ₂ Mo ₂ S ₂ (CO) ₈	2.789(av)	2.362(av)	2.213(2)		9d
(MeCp) ₂ Fe ₂ Mo ₂ (CO) ₆ S ₄	2.853(3)	2.425(av)	2.234(av)		30
(MeCp) ₂ Fe ₂ Mo ₂ (CO) ₆ S ₃	2.803(av)	2.352(av)	2.389(av)		30
(MeCp) ₂ Mo ₂ S ₄ FeCp	2.779(av)	2.406(av)	2.130(av)		30
Cp* ₂ FeMo ₂ S ₄ (CO) ₂	2.777(av)	2.438(av)	2.153(1)		31
Cp* ₂ FeMo ₂ S ₄ (CO) ₃	2.824(av)	2.463(av)	2.130(1)		31
Cp* ₂ Fe ₂ Mo ₂ S ₄ (CO) ₄	2.813(av)	2.323(av)	2.271(av)		31
Fe ₂ W(CO) ₉ (PMe ₂ Ph) ₂ S ₂	2.776(av)	2.424(av)	2.252(av)		11a
Fe ₃ W(CO) ₁₁ (PMe ₂ Ph) ₂ S ₂	2.772(av)	2.379(av)	2.192(av)	2.562(av)	11a
Fe ₂ W(CO) ₁₁ S	2.853(av)	2.429(2)	2.179(av)	2.569(2)	3b
Fe ₂ W(CO) ₁₀ (PMe ₂ Ph)S	2.815(av)	2.406(2)	2.187(av)	2.572(1)	3b
Cp ₂ W ₂ Fe(CO) ₇ S	2.800(av)	2.358(av)	2.204(7)		32

metal–metal interaction exists (Table 3).^{26,29} The average bond distances of Mo–Fe (2.8206 Å), W–Fe (2.7832 Å), Mo–S (2.4302 Å), W–S (2.3214 Å), Fe–S (2.2398 Å), and Fe–Fe (2.5414 Å) are also comparable with the reported values (Table 4).^{3b,9b,d,11a,30–32} In general, in these clusters the Mo–S_{br} (2.4302 Å, av) and Mo–P_{br} (2.4806 Å, av) distances are longer than the W–S_{br} (2.3214 Å, av) and W–P_{br} (2.4346 Å, av) distances, respectively, and in accord with the literature values.^{10,20–22} The Fe–C_{tr} (2.0345 Å, av) is longer than the Fe–C_{tr} (1.7553 Å, av) in **1**, **3**, **5**, and **6**.

Conclusions

This paper describes the reactivity of Fe₂(μ-S₂)(CO)₆ toward heterodinuclear phosphido-bridged Cp(CO)₂-W(μ-PPh₂)Mo(CO)₅ and Fe₂(μ-S₂)(CO)₆ under mild conditions. A new reactivity pattern is shown by Fe₂(μ-S₂)(CO)₆, where it is unusually fragmented to FeS₂(CO)₃ and Fe(CO)₃ to form **2**, and also coordinated to **3** in a unique mode. Clusters **1** and **2** are important additions to the reaction chemistry of Fe₂(μ-S₂)(CO)₆ with metal–metal dinuclear complexes. The bridging phosphido ligand may confer extra stability in **1** and **2** and facilitate their isolation.

Experimental Section

General Procedures. Reactions were carried out under an atmosphere of nitrogen using standard Schlenk techniques. All commercially available chemicals were purchased and used as received. Solvents were dried and distilled under nitrogen using standard methods. Compounds Cp(CO)₂W(μ-PPh₂)Mo(CO)₅, Fe₃(μ-S)₂(CO)₉, and Fe₂(μ-S₂)(CO)₆ were prepared following reported procedures.^{1b,10} Infrared spectra were obtained on a Perkin-Elmer 882 infrared spectrophotometer. The ¹H and ³¹P NMR spectra were recorded on a Bruker Ac-300 spectrometer. ³¹P NMR shifts are referenced to 85% H₃PO₄. Microanalyses were obtained on a Perkin-Elmer 2400 CHN analyzer.

Reaction of Cp(CO)₂W(μ-PPh₂)Mo(CO)₅ with Fe₂(μ-S₂)(CO)₆. To a solid mixture of Cp(CO)₂W(μ-PPh₂)Mo(CO)₅ (400 mg, 0.55 mmol) and Fe₂(μ-S₂)(CO)₆ (300 mg, 0.87 mmol) was added dichloromethane (50 mL) and the mixture kept at reflux

for about 20 h. The reaction mixture was filtered through Celite to remove the insoluble material and the filtrate evaporated to dryness. The residue was then dissolved in dichloromethane (10 mL), and the solution was subjected to chromatography using a silica gel column (45 cm × 3.5 cm). Elution with a dichloromethane and hexane (1:4) mixture collected three fractions. The first, violet fraction was a mixture of the known compound Fe₃(μ-S)₂(CO)₉ and starting material Fe₂(μ-S₂)(CO)₆. They were further separated by chromatography with a long silica gel column (100 cm × 2.5 cm) using hexane as an eluent. The first, orange band gave Fe₂(μ-S₂)(CO)₆, and the second, violet band was Fe₃(μ-S)₂(CO)₉. The second fraction was a mixture of starting material Cp(CO)₂-

W(μ-PPh₂)Mo(CO)₅ and **1**. They were further separated by silica gel column (45 cm × 2.5 cm) chromatography using a mixture of hexane, dichloromethane, and ethyl acetate (8:1:1) as eluent. The first, violet band was Cp(CO)₂W(μ-PPh₂)Mo(CO)₅ followed by a second, dirty green band, which was **1**. The third fraction was brown in color. The brown solid obtained was further separated by silica gel column (60 cm × 2.5 cm) chromatography with a mixture of hexane, dichloromethane, and ethyl acetate (8:1:1) as the eluent. Three bands were obtained. Clusters **4**, **3**, and **2**, were obtained from the first, dirty green, the second, reddish brown, and the third, brown bands, respectively. **1**: Yield: 67 mg, 15%. Anal. Calcd for C₂₆H₁₅O₉PS₂Fe₂MoW: C, 32.57; H, 1.57. Found: C, 32.73; H, 1.86. IR (CH₂Cl₂): ν(CO) 2047 (s), 2013 (vs), 1994 (m), 1964 (w, sh), 1943 (w, sh), 1855 (w, br) cm⁻¹. ¹H NMR (CDCl₃): δ 7.84–7.38 (m, 10H, C₆H₅), 5.19 (s, 5H, C₅H₅). ³¹P{¹H} NMR (CH₂Cl₂): δ 177.3 (s). **2**: Yield: 27 mg, 7%. Anal. Calcd for C₂₄H₁₅O₇PS₂FeMoW: C, 34.04; H, 1.77. Found: C, 33.79; H, 1.74. IR (CH₂Cl₂): ν(CO) 2060 (s), 2001 (vs), 1984 (w, sh), 1938 (w, sh) 1915 (m) cm⁻¹. ¹H NMR (CDCl₃): δ 7.81–7.23 (m, 10H, C₆H₅), 5.67 (s, 5H, C₅H₅). ³¹P{¹H} NMR (CH₂Cl₂): δ 115.1 (s). **3**: Yield: 114 mg, 27%. Anal. Calcd for C₂₅H₁₅O₈PS₂Fe₂MoW: C, 32.22; H, 1.61. Found: C, 32.41; H, 1.63. IR (CH₂Cl₂): ν(CO) 2053 (s), 2007 (vs), 1954 (s), 1810 (m) cm⁻¹. ¹H NMR (CDCl₃): δ 7.44–7.34 (m, 10H, C₆H₅), 5.65 (s, 5H, C₅H₅). ³¹P{¹H} NMR (CH₂Cl₂): δ 25.0 (s). **4**: Yield: 17 mg, 3%. Anal. Calcd for C₂₈H₁₅O₁₁PS₄Fe₄MoW: C 28.24, H 1.26. Found: C 28.35, H 1.43. IR (CH₂Cl₂): ν(CO) 2080 (s), 2049 (vs), 2018 (m), 1995 (w), 1979 (m), 1950 (m), 1758 (vw) cm⁻¹. ¹H NMR (CDCl₃): δ 7.54–7.35 (m, 10H, C₆H₅), 5.64 (s, 5H, C₅H₅). ³¹P{¹H} NMR (CH₂Cl₂): δ 267.6 (s). The yield is calculated on the basis of reacted Cp(CO)₂W(μ-PPh₂)Mo(CO)₅ (334 mg, 0.46 mmol).

Thermolysis of 1 in Dichloromethane. A dichloromethane solution (25 mL) of **1** (60 mg, 0.063 mmol) was kept at reflux for 20 h, and then the reaction mixture concentrated to 5 mL. Silica gel column (45 cm × 2.5 cm) chromatography using a mixture of hexane and dichloromethane (3:2) as the eluent gave **3**. Yield: 45 mg, 77%.

Thermolysis of 1 in the Presence of Fe₂(μ-S₂)(CO)₆. A dichloromethane solution (10 mL) of **1** (30 mg, 0.031 mmol)

(29) Miriam, B.; Lima, G. D.; Guerschais, J. E.; Mercier, R.; Pétillon, F. Y. *Organometallics* **1986**, *5*, 1952.

(30) Cowans, B. A.; Haltiwanger, R. C.; DuBois, M. R. *Organometallics* **1987**, *6*, 995.

(31) Brunner, H.; Jnietz, N.; Wachter, J.; Zahn, T.; Ziegler, M. L. *Angew. Chem., Int. Ed. Engl.* **1985**, *24*, 133.

(32) Williams, P. D.; Curtis, M. D. *J. Organomet. Chem.* **1988**, *352*, 169.

and $\text{Fe}_2(\mu\text{-S}_2)(\text{CO})_6$ (20 mg, 0.059 mmol) was refluxed for 8 h. The reaction mixture was concentrated to 5 mL, and three fractions were collected by silica column (60 cm \times 2.5 cm) chromatography using hexane and dichloromethane (8:2) as an eluent. Unreacted $\text{Fe}_2(\mu\text{-S}_2)(\text{CO})_6$ (17 mg, 85% yield) was isolated from the first, orange fraction with a trace of $\text{Fe}_3(\mu\text{-S})_2(\text{CO})_9$ by TLC in hexane. The second, dirty green fraction was unreacted **1** (5 mg, 17% yield). The third, reddish brown fraction gave **3** (17 mg, 71% yield) with a trace of **2** by TLC workup in a mixture of hexane, dichloromethane, and ethyl acetate (8:1:1). The yield was calculated on the basis of consumed **1**.

Reaction of **2 with $\text{Fe}_2(\text{CO})_9$.** To a dichloromethane solution (25 mL) of **1** (50 mg, 0.06 mmol) was added $\text{Fe}_2(\text{CO})_9$ (110 mg, 0.3 mmol) and refluxed for 20 h. The reaction mixture was concentrated to 5 mL, and then silica gel column (45 cm \times 2.5 cm) chromatography using a mixture of hexane, dichloromethane, and ethyl acetate (8:1:1) as an eluent gave three bands. The first unidentified band was trace in amount and yellow in color. The second, reddish brown band was **3** (11 mg, 29% yield), and the third, brown band was unreacted **2**. The yield of **3** was calculated on the basis of reacted **2** (30 mg, 0.04 mmol).

Reaction of $\text{Cp}(\text{CO})_2\text{W}(\mu\text{-PPh}_2)\text{Mo}(\text{CO})_5$ with $\text{Fe}_3(\mu\text{-S})_2(\text{CO})_9$. A solid mixture of $\text{Cp}(\text{CO})_2\text{W}(\mu\text{-PPh}_2)\text{Mo}(\text{CO})_5$ (100 mg, 0.14 mmol) and $\text{Fe}_3(\mu\text{-S})_2(\text{CO})_9$ (100 mg, 0.21 mmol) was dissolved in 50 mL of dichloromethane. The mixture was refluxed for 20 h. The reaction mixture was concentrated to 5 mL, which was then subjected to chromatography using a silica gel column (45 cm \times 2.5 cm) with a mixture of hexane and dichloromethane (4:1) as the eluent. Compounds $\text{Fe}_3(\mu\text{-S})_2(\text{CO})_9$ (93 mg, 93% yield) and $\text{Cp}(\text{CO})_2\text{W}(\mu\text{-PPh}_2)\text{Mo}(\text{CO})_5$ (97 mg, 97% yield) were obtained from the first, violet and the second, violet bands, respectively. Both complexes were identified by comparing their IR and $^{31}\text{P}\{^1\text{H}\}$ NMR spectra with the literature data.^{1b,10}

Reflux of $\text{Fe}_2(\mu\text{-S}_2)(\text{CO})_6$ in Dichloromethane. A dichloromethane solution (25 mL) of $\text{Fe}_2(\mu\text{-S}_2)(\text{CO})_6$ (100 mg, 0.29 mmol) was kept at reflux for 20 h. Silica gel column (45 cm \times 2.5 cm) chromatography of the concentrated reaction mixture (5 mL) using hexane as an eluent recovered 95 mg (95% yield) of $\text{Fe}_2(\mu\text{-S}_2)(\text{CO})_6$.

Reaction of **3 with $\text{Fe}_2(\mu\text{-S}_2)(\text{CO})_6$.** To a mixture of **3** (80 mg, 0.09 mmol) and $\text{Fe}_2(\mu\text{-S}_2)(\text{CO})_6$ (45 mg, 0.13 mmol) was added 50 mL of dichloromethane and refluxed for 20 h. The reaction mixture was concentrated to 5 mL, and then chromatographic workup (silica gel column) using hexane and dichloromethane (3:1) as an eluent afforded the first, orange band, $\text{Fe}_2(\mu\text{-S}_2)(\text{CO})_6$ (42 mg, 93% yield), and the second, reddish brown band, **3** (78 mg, 97% yield), respectively.

Reaction of **3 with Norbornadiene.** To a benzene solution (50 mL) of **3** (50 mg, 0.053 mmol) was added nbd (25 mg, 0.27 mmol) and then refluxed for 30 h. The reaction mixture was evaporated to dryness. The residue was then dissolved in

dichloromethane and concentrated to 5 mL. The cluster **5** was collected as a brown band on silica gel column (45 cm \times 2.5 cm) chromatography using dichloromethane and hexane (1:1) as an eluent. Yield: 16 mg, 31%. Anal. Calcd for $\text{C}_{30}\text{H}_{23}\text{O}_6\text{-PS}_2\text{Fe}_2\text{MoW}$: C, 37.26; H, 2.38. Found: C, 37.34; H, 2.42. IR (CH_2Cl_2): $\nu(\text{CO})$ 2006 (vs), 1978 (s), 1940 (s), 1828 (m), 1797 (w, sh) cm^{-1} . ^1H NMR (CDCl_3): δ 7.68–7.23 (m, 10H, C_6H_5), 5.50 (s, 5H, C_5H_5), 5.65 (br, 2H, nbd), 4.40 (br, 2H, nbd), 3.88 (br, 2H, nbd), 1.4 (br 2H, nbd). $^{31}\text{P}\{^1\text{H}\}$ NMR (CH_2Cl_2): δ 27.1 (s).

Thermolysis of **3 in Benzene.** A benzene solution (50 mL) of **3** (60 mg, 0.064 mmol) was refluxed for 34 h. The solution was evaporated to dryness. The residue was then dissolved in dichloromethane and concentrated to 5 mL. The cluster **6** was collected as a reddish band on silica gel column (45 cm \times 2.5 cm) chromatography using dichloromethane and hexane (1:1) as an eluent. Yield: 22 mg, 37%. Anal. Calcd for $\text{C}_{28}\text{H}_{21}\text{O}_5\text{-PS}_2\text{Fe}_2\text{MoW}$: C, 36.36; H, 2.27. Found: C, 36.25; H, 2.31. IR (CH_2Cl_2): $\nu(\text{CO})$ 1986 (vs), 1958 (s), 1922 (s), 1751 (m) cm^{-1} . ^1H NMR (CDCl_3): δ 7.37–7.29 (m, 10H, C_6H_5), 5.40 (s, 5H, C_5H_5), 5.20 (s, 6H, C_6H_6). $^{31}\text{P}\{^1\text{H}\}$ NMR (CH_2Cl_2): δ -6.2 (s).

Crystal Structure Determination of Clusters 1–6. Individual solutions of compounds **1–5** in dichloromethane were layered by hexane first. The single crystals of **1–5** for X-ray diffraction analyses were grown by slow evaporation of these mixtures at 0 °C, respectively. A single crystal of **6** was obtained similarly by slow evaporation of its dichloromethane solution layered by toluene at 0 °C. For each of the clusters **1–6**, a selected single crystal was mounted on a glass fiber for data collection by using Mo $\text{K}\alpha$ radiation on an Enraf Nonius CAD4 diffractometer at room temperature. Table 1 gives further details. Unit cell parameters were refined from 25 reflections with the 2θ range 14.52–35.92°. Three standard reflections were monitored every hour throughout the data collection. The variation was within 6%. Lorentz and polarization corrections were applied. A semiempirical absorption correction was applied based on azimuthal scans of three reflections. All structures were solved by direct methods. For all hydrogen atoms, the atomic and isotropic thermal parameters were fixed. Structure refinement was performed using the Wingx³³ program on a PC.

Acknowledgment. We acknowledge the National Science Council of the Republic of China and Academia Sinica for financial support of this work.

Supporting Information Available: Tables of atomic coordinates, isotropic and anisotropic displacement parameters, and all bond distances and angles, and experimental details of the X-ray studies for **1–6**. This material is available free of charge via the Internet at <http://pubs.acs.org>.

OM049821T

(33) Farrugia, L. J. *J. Appl. Crystallogr.* **1999**, *32*, 837.